ISDRS 2013, December 11-13. 2013

# NiGe/$n^+$Ge Junctions with Record-low Contact Resistivity (~$3\times10^{-8}$ Ωcm$^2$) Formed by Two-step P-ion Implantation

Masahiro Koike, Yuuichi Kamimuta, Etsuo Kurosawa, and Tsutomu Tezuka
*Green Nanoelectronics Center* (*GNC*), *National Institute of Advanced Industrial Science and Technology* (*AIST*),
*Japan,* massahiro.koike@aist.go.jp

To realize Ge *n*MOSFETs with metal contacts on $n^+$Ge S/D junctions, such as NiGe/$n^+$Ge junctions, a large Schottky barrier height (SBH) of ~0.6 eV, resulting in a high contact resistivity ($\rho_C$), is an issue that remains to be resolved [1,2]. The high $\rho_C$ is due to the Fermi level pinning of NiGe close to the valence band maximum of Ge. One way to resolve this issue is to increase the electron concentration of P at the NiGe/Ge interface, leading to a reduced effective SBH. In this study, we have fabricated NiGe/$n^+$Ge junctions by two-step P-ion implantation to intentionally increase the impurity concentration ($N_B$) of P at the NiGe/*n*Ge interface while keeping a low drain leakage current in Ge *n*MOSFETs. Using this technique, an ultralow $\rho_C$ of ~$3\times10^{-8}$ Ω cm$^2$ and an $I_F/I_R$ ratio of over $10^6$ were demonstrated.

NiGe/$n^+$Ge junctions were fabricated as follows. P ions were implanted (1st P I/I) into *p*Ge(100) with $SiO_2$ isolation at an acceleration energy ($E_A$) of 20 keV, followed by annealing at 600$^o$C for 1 min to form $n^+$Ge/*p*Ge(100). After annealing, P ions were again implanted (2nd P I/I) into the $n^+$Ge at $E_A$ of 10 and 20 keV, where the doses were respectively $1\times10^{15}$ and $1.65\times10^{15}$ cm$^{-2}$, to achieve the same peak value of $N_B$ for P. Then, a Ni film with a thickness of 5 or 10 nm was deposited. After germanidation annealing at 350$^o$C in $N_2$ for 1 min, the wafers were treated with HCl solution to remove unreacted Ni, which was followed by Ti deposition. As references, NiGe/$n^+$Ge without the second P I/I or Ni deposition or both were also fabricated; in the case without Ni deposition, Ti/$n^+$Ge was fabricated. The value of $\rho_C$ for NiGe/$n^+$Ge was determined by the transfer length method (TLM).

Simulated profiles of P in Ge after P I/I at $E_A$ of 10 and 20 keV corresponding to the 2nd I/I show that the peak $N_B$ was as high as ~$5\times10^{20}$ cm$^{-3}$ (Fig. 1). On the other hand, we confirmed experimentally that the profiles of $n^+$Ge with the 1st P I/I Ge after annealing at 600$^o$C had a boxlike shape (~100 nm), where the maximum $N_B$ for P was as low as ~$2\times10^{19}$ cm$^{-3}$ (Fig. 1). Therefore, NiGe/$n^+$Ge with the 2nd P I/I is expected to have a high $N_B$ (~$5\times10^{20}$ cm$^{-3}$) at the interface. Next, we observed the $n^+$Ge region in NiGe/$n^+$Ge by TEM. The TEM images of NiGe/$n^+$Ge with and without the 2nd P I/I revealed similar structures (Fig. 2), indicating that the amorphous phase due to the 1st and 2nd P I/I disappeared as a result of annealing at 600 and 350$^o$C, respectively. The *J-V* characteristics show that the junction leakage currents of NiGe/$n^+$/*p*Ge were considerably suppressed irrespective of the 2nd P I/I (Fig. 3). This is because the residual crystalline defects due to the 2nd I/I were completely confined in the deep $n^+$ region formed by the 1st I/I and the high-temperature annealing. A junction formed by only the 2nd P I/I and the germanidation process exhibited no rectifying characteristics owing to the residual crystalline defects. On the other hand, the value of *J* between the two metal contacts in the TLM structures was higher in NiGe/$n^+$Ge/NiGe with the 2nd P I/I than without the 2nd P I/I (Fig. 4). To determine the value of $\rho_C$, we measured the NiGe/$n^+$Ge/NiGe structure with various contact spacings in the TLM structure. Figure 5 shows the relationship between the contact spacing and the total resistance for NiGe/$n^+$Ge with and without the 2nd P I/I. Whereas the similar slopes of the two relationships suggest almost the same sheet resistivity ($\rho sh$), the different intercept values suggest that NiGe/$n^+$Ge with the 2nd P I/I has a lower $\rho_C$ than that without the 2nd P I/I. We summarize the average $\rho_C$ for NiGe/$n^+$Ge as functions of the Ni thickness and P dose (Fig. 6). Whereas $\rho_C$ for NiGe/$n^+$Ge (Ti/$n^+$Ge) without the 2nd P I/I gradually decreased with increasing Ni thickness, $\rho_C$ for the junctions with the 2nd P I/I rapidly decreased. $\rho_C$ for the NiGe/$n^+$Ge junction fabricated with the 2nd P I/I and 10 nm Ni layer exhibited an ultralow value of ~$3\times10^{-8}$ Ωcm$^2$. We found that $\rho_C$ was strongly correlated with $N_B$ for P at the NiGe/Ge interface (Fig. 7), which was expected from the simulated profiles of P-implanted Ge (Fig. 1). According to the calculated $\rho_C$ on *n*Si(100) for an SBH of 0.6 eV, a change in $N_B$ from $3\times10^{19}$ to $2\times10^{20}$ cm$^{-3}$ results in a change in $\rho_C$ from $3\times10^{-5}$ to $3\times10^{-8}$ Ωcm$^2$ [3]. Thus, the change in $\rho_C$ from $3\times10^{-5}$ to $3\times10^{-8}$ Ωcm$^2$ for NiGe/$n^+$Ge can be explained by the increase in $N_B$ around the NiGe/$n^+$Ge interface owing to the 2nd P I/I. This result suggests that the P atoms existing around the NiGe/$n^+$Ge interface after the 2nd P I/I were electrically active in spite of the low annealing temperature of 350$^o$C, which is usually insufficient to activate P in bulk Ge. Finally, we compare $\rho c$ values for previously reported metal/$n^+$Ge junctions with our result (Table 1). The NiGe/$n^+$Ge contact in this work has the lowest $\rho c$. From these results, the fabrication of NiGe/$n^+$Ge by two-step P-ion implantation is an effective means of obtaining metal contacts on S/D junctions with a low $\rho c$ in Ge *n*MOSFETs.

We would like to thank all the technical staff of AIST for supporting our experiment. This work was supported by a grant from JSPS through the FIRST Program initiated by CSTP.

## References

[1] M. Koike et al., *Appl. Phys. Express* **4**, 021301 (2011). [2] M. Koike et al., *Appl. Phys. Lett.*, **102**, 032108 (2013). [3] S. M. Sze, *Physics of Semiconductor Devices, 2nd ed.* (Wiley-Interscience, New York, 1981). [4] M. Shayesteh et al., *Electron Dev.* **58**, 3801 (2011). [5] K. Mrtens et al., *Tech. Dig. IEDM*, 18.4 (2010). [6] S. Raghunathan et al., *ECS Trans.* **33**, 871, (2010). [7] G. Thareja et al., *Electron Dev. Lett.*, **32**, 608 (2010). [8] K. Gallacher et al., *ECS Trans*, **50**, 1081 (2012).

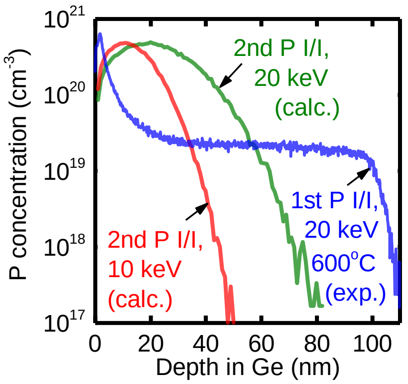

Fig. 1: Profiles of P in Ge.

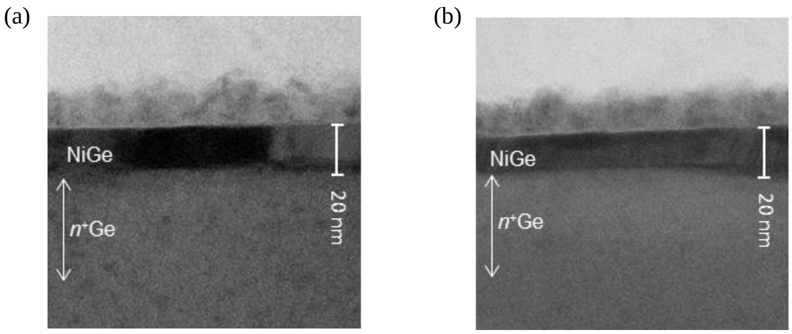

Fig. 2: TEM images of NiGe/$n^+$Ge junctions (a) with 2nd P I/I and (b) without 2nd P I/I. NiGe (~20 nm) was fabricated by annealing Ni (10 nm)/$n^+$Ge.

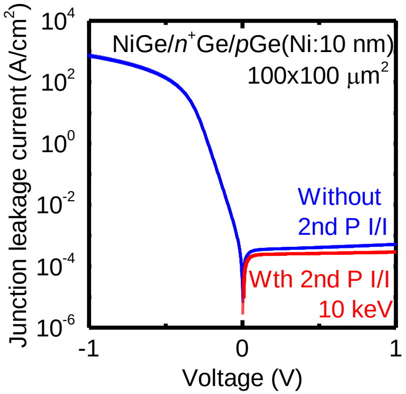

Fig. 3: *J*-*V* characteristics of NiGe /*n*+/*p*Ge junctions in TLM structures.

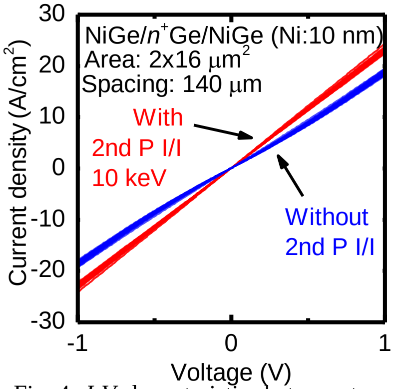

Fig. 4: *J*-*V* characteristics between two contacts (NiGe /$n^+$Ge/NiGe) in TLM structures.

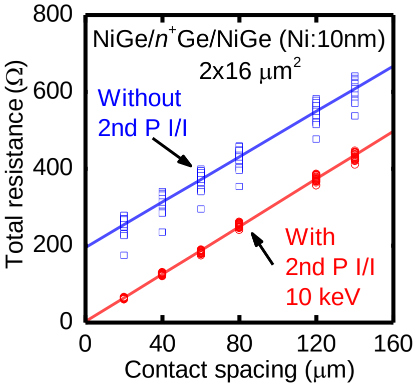

Fig. 5: Relationship between NiGe contact spacing and total resistance including $\rho c$ and $\rho sh$ in TLM structures.

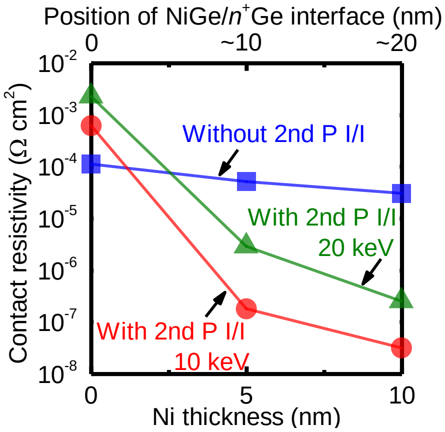

Fig. 6: Contact resistivities of NiGe/$n^+$Ge junctions in TLM structures.

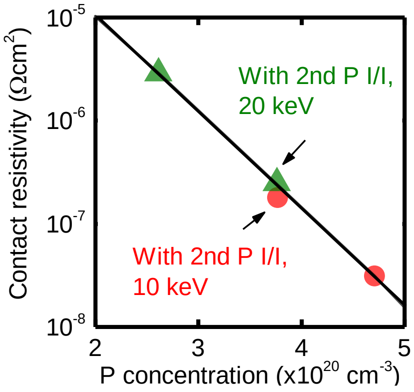

Fig. 7: Relationship between measured contact resistivity and calculated concentration of P at the NiGe/$n^+$Ge interface.

Table 1: Contact resistivity values reported for metal/$n^+$Ge junctions.

| Metal | Doping | Activation anneal (°C) | NiGe formation (°C) | $\rho c$ (Ω$cm^2$) | |
|---|---|---|---|---|---|
| NiGe | P | 500 | 250 | $3.46\times10^{-6}$ | [4] |
| NiGe | As | 900(LSA) | 250/330 | $2.5\times10^{-6}$ | [5] |
| NiGe | P/Sb | | 500 | $8\times10^{-7}$ | [6] |
| Al/Ti | Sb | LSA | | $7\times10^{-7}$ | [7] |
| NiGe | P | | 2step<br>250-340/340 | $1.68\times10^{-7}$ | [8] |
| NiGe | 2step P | 600 | 350 | $3\times10^{-8}$ | This work |